

## Full Articles

### Intra- and inter-ring haptotropic rearrangements in (naphthalene and anthracene)nickel complexes: a DFT study

Yu. F. Oprunenko\* and I. P. Gloriov

Department of Chemistry, M. V. Lomonosov Moscow State University,  
Bldg. 3, 1 Leninskie Gory, 119991 Moscow, Russian Federation

Fax: +7 (495) 939 26 77. E-mail: oprunenko@nmr.chem.msu.ru, gloriov@nmr.chem.msu.ru

Density functional quantum chemical calculations of the mechanisms of metallotropic  $\eta^2, \eta^2$ -intra- and  $\eta^2, \eta^2$ -inter-ring haptotropic rearrangements (HRs) in 16e zero-valent  $\eta^2$ -(naphthalene and anthracene)nickel complexes involving migration of the organometallic group within the same ring or from one aromatic ring to the other were carried out. The structures of the initial complexes, transition states, and intermediates were determined. The intra-ring HRs in these systems proceed *via* low-energy  $\eta^4$ -*cis*-butadiene transition states. The inter-ring HRs proceed along the periphery of the naphthalene and anthracene ligands *via* high-energy  $\eta^3$ -allylic transition states. In contrast to well-investigated  $\eta^6, \eta^6$ -inter-ring HRs in (naphthalene and anthracene)tricarbonylchromium complexes, the activation barriers to the  $\eta^2, \eta^2$ -inter-ring HRs in the corresponding nickel complexes are much lower. Transition states of these processes are characterized by higher hapticity compared to the initial complexes. This also distinguishes the nickel complexes from the corresponding  $\text{Cr}(\text{CO})_3$  complexes for which the hapticities of transition states of the  $\eta^6, \eta^6$ -inter-ring HRs are lower than those of the initial complexes. The calculated activation barriers to the  $\eta^2, \eta^2$ -intra-ring HRs in the (naphthalene and anthracene)nickel complexes as well as the barrier to rotation of the organonickel group in the naphthalene complex are in good agreement with the experimental data. The calculated barriers to the  $\eta^2, \eta^2$ -inter-ring HRs in the naphthalene and anthracene complexes are 3–5 kcal mol<sup>–1</sup> lower than the experimental values. This is probably due to the competition between two mechanisms of this process, a low-energy intramolecular mechanism and a high-energy intermolecular dissociative mechanism.

**Key words:** density functional theory, PBE functional, quantum chemical calculations, nickel complexes, polyaromatic ligands, transition states, intermediates.

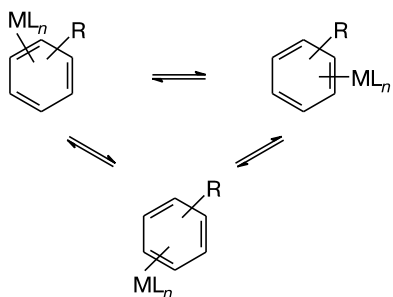
Transition metal complexes with aromatic ligands are of significant interest owing to specific features of their structures as well as dynamic properties.<sup>1</sup> Recently,

the ability of such complexes to catalyze many organic reactions<sup>2</sup> and to activate some positions in the ligands, which can be used in the synthesis of difficult-

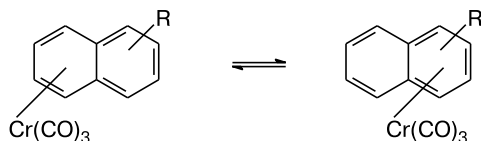
to-access organic derivatives,<sup>3</sup> has become of practical value.

Among dynamic processes in such complexes, intra-ring<sup>4</sup> and inter-ring<sup>5</sup> haptotropic rearrangements (HRs) shown in Schemes 1 and 2, respectively, have become a subject of intensive recent studies. These processes involve intramolecular migration of the metal atom with its ligand environment (*i*) within the same ring or (*ii*) along the perimeter of a polycyclic carbocycle<sup>6</sup> (naphthalene, biphenyl, *etc.*) or heterocycle<sup>7</sup> (dibenzothiophene, carbazole, *etc.*) from one ring to the other.

Scheme 1



Scheme 2



Intra-ring HRs in complexes with unsaturated ligands are usually characterized by low activation barriers and often studied by dynamic NMR spectroscopy. Such processes are particularly characteristic of the broad class of transition metal complexes with cyclopolyenes, *e.g.*, cyclo-octatetraene (COT).<sup>8,9</sup>

Thorough modern-level studies of the  $\eta^4, \eta^4$ -intra-ring HR in an (COT)osmium complex were carried out by 2D NMR spectroscopy (EXSY). It was proved that the rearrangement proceeds by the [1,2]-M-shift mechanism. The experimentally determined activation barrier is  $E_a = 5.9 \text{ kcal mol}^{-1}$ . According to the density functional theory (DFT) calculations, the rearrangement of the osmium complex proceeds *via* a nonplanar symmetric  $\eta^3$ -transition state with the osmium atom bound to three carbon atoms. The calculated activation barrier to the reaction approaches the experimental value ( $E_a = 6.5 \text{ kcal mol}^{-1}$ ).<sup>10</sup>

The structures of the ( $\eta^2$ -COT)manganese and -iron complexes  $\text{CpMn}(\text{CO})_2(\eta^2\text{-C}_8\text{H}_8)$  (see Ref. 11) and  $[\text{CpFe}(\text{CO})_2(\eta^2\text{-C}_8\text{H}_8)]\text{PF}_6$  (see Ref. 12) display no dynamic processes in the corresponding thermal stability ranges. Nevertheless, a more recent study<sup>8</sup> showed that

the statement that all  $\eta^2$ -complexes of COT are static<sup>13</sup> is not always correct. For instance, in the complexes  $(\text{R}_2\text{PC}_2\text{H}_4\text{PR}_2)\text{Ni}(\eta^2\text{-C}_8\text{H}_8)$  ( $\text{R} = \text{Pr}^i, \text{Bu}^i$ ) the organonickel group very rapidly migrates within the ring through [1,3]-metal shifts. The limiting spectrum is not observed even at 173 K. It follows that the activation barrier to  $\eta^2, \eta^2$ -intra-ring HR is at most  $5 \text{ kcal mol}^{-1}$ . It was assumed<sup>14</sup> that the rearrangement proceeds *via* a transition state with a higher hapticity compared to that of the initial complex ( $\eta^4$  vs.  $\eta^2$ , respectively). Intra-ring HRs in complexes with various cyclopolyolefins may proceed by the [1,2]- or [1,3]-metal shift mechanisms;<sup>15</sup> in addition,  $\eta^2, \eta^2$ -intra-ring HRs may proceed as combinations of these two processes.<sup>15,16</sup>

Dynamic behavior is also characteristic of transition metal complexes with monocyclic arene ligands (*e.g.*, benzene and hexafluorobenzene, see Scheme 1), especially when not all unsaturated bonds are involved in coordination with the metal atom. Among such complexes, a particular place is occupied by  $\eta^2$ -complexes of transition metals, *e.g.*, Ni,<sup>4</sup> Os,<sup>17</sup> Rh,<sup>18</sup> Re,<sup>19</sup> *etc.* Complexes with polyaromatic ligands (*e.g.*, naphthalene, anthracene, octafluoronaphthalene) were also reported. They also exhibit  $\eta^2, \eta^2$ -intra-ring HRs (see Refs 20–22) with low activation barriers ( $5\text{--}10 \text{ kcal mol}^{-1}$ ), which can be studied by dynamic NMR spectroscopy. Some rhodium<sup>21</sup> and iridium<sup>22</sup> complexes with  $\text{C}_6\text{F}_6$  show no dynamic behavior.

The known  $\eta^6, \eta^6$ - or  $\eta^6, \eta^5$ -inter-ring HRs have been best studied experimentally for transition metal complexes with polyaromatic ligands (*e.g.*, neutral and anionic complexes of fluorene, azafluorenes, and some other polyaromatic ligands with fused five- and six-membered rings). The activation parameters of both intra-ring and inter-ring HRs in these systems depend on various factors, but the latter processes are usually characterized by much higher barriers ( $28\text{--}35 \text{ kcal mol}^{-1}$ ) and can be studied by spectroscopic methods.

To compare with experimental data we, as well as other authors, carried out DFT calculations of inter-ring HRs in (naphthalene, biphenyl, biphenylene, dibenzothiophene, anthracene, phenanthrene, and fluoranthene)-tricarboxylchromium complexes and in some other  $\text{Cr}(\text{CO})_3$  complexes with polyaromatic ligands<sup>23–25</sup> including such complex systems as coronene<sup>26</sup> and nanotubes.<sup>27</sup> Calculations provide a quite correct description of the geometric parameters (distances, angles, conformations of the tricarboxylchromium group relatively to aromatic ligands) of these stable complexes obtained in X-ray diffraction, gas-phase electron diffraction, and gas-phase neutron diffraction studies. The applicability of DFT to modeling of intermediates and transition states is confirmed by good agreement between the theoretical and experimental kinetic and thermodynamic parameters of inter-ring HRs.

A large number of haptotropic rearrangements in aromatic polycycles were disclosed and qualitatively studied<sup>5,23</sup> for many other transition metals including Mo, W, Rh, Pd, Ir, Ni, Mn, Fe, Zr, Ru, and Os. For most of them, DFT calculations have not been carried out because the activation barriers to such rearrangements (determined from reliable kinetic data) are unknown; which reduces interest in their theoretical description. Nevertheless, there are few rearrangements in some metal (other than chromium) complexes that were studied experimentally and/or theoretically. An illustration is provided by the  $\eta^2, \eta^2$ -intra-ring HRs and  $\eta^2, \eta^2$ -inter-ring HRs in the Rh, Co, and Ru ( $\eta^2$ -C<sub>60</sub> fullerene) complexes. The organometallic group migrates across the fullerene surface by means of [1,3]-shifts<sup>28</sup> characterized by the barriers  $\Delta G^\ddagger_{\text{exp}}$  of about 9 (Rh), 10 (Co), and 14 (Ru) kcal mol<sup>-1</sup>.

A  $\eta^6, \eta^5$ -inter-ring HR in the cyclopentadienylium complex of fluorenyl anion was studied experimentally by electronic spectroscopy in hexane<sup>29</sup> ( $\Delta G^\ddagger_{\text{exp}} \approx 22.5$  kcal mol<sup>-1</sup>) and by NMR spectroscopy in benzene<sup>30</sup> ( $\Delta G^\ddagger_{\text{exp}} \approx 31$  kcal mol<sup>-1</sup>) as well as theoretically ( $\Delta G^\ddagger_{\text{DFT}} \approx 27.3$  kcal mol<sup>-1</sup>, B3LYP calculations<sup>30</sup>). The large scatter of experimental values is noteworthy. This is probably due to strongly different concentrations of the complexes in the kinetic measurements by electronic spectroscopy and by NMR spectroscopy, as well as by the fact that the rearrangements were carried out in the solvents with strongly different properties. In principle, gas-phase calculations should give better results for the inter-ring HR in inert, non-solvating, and non-coordinating hexane at high dilution compared to the inter-ring HR in benzene, which readily reacts with organometallic substrates, taking into account a higher substrate concentration necessary for NMR measurements.

However, it should be noted that the theoretical estimate falls between two experimental values. Methods of taking into account the solvent effect on the gas-phase thermodynamic parameters of organometallic reactions obtained from DFT calculation have not been well developed as yet, are time-consuming and used rarely. The fact that the results of calculations of haptotropic rearrangements are in good fit to the experimental data indicates that gas-phase calculations quite correctly describe reactions in solutions in inert, non-coordinating and non-solvating solvents (*e.g.*, hexane or hexafluorobenzene).<sup>5–7</sup>

$\eta^4, \eta^4$ -Inter-ring HRs in ( $\eta^4$ -ethylnaphthalene)iridium complexes were studied by NMR spectroscopy ( $\Delta G^\ddagger_{283\text{ K}} \approx 21$  kcal mol<sup>-1</sup>).<sup>31</sup> Recently, we have reported a DFT study of these processes.<sup>32</sup>

The aforesaid suggests that the intra-ring and inter-ring HRs are very sensitive to minor changes in the structure of aromatic ligands,<sup>5–7,26,27</sup> the presence or absence of heteroatoms,<sup>7,23</sup> the charge distribution,<sup>23</sup> the type of extra ligands L,<sup>5,25</sup> the nature of the metal,<sup>26,28</sup> the aggregation state,<sup>20,23</sup> and the polarity of the reaction medi-

um.<sup>23,31,32</sup> Systematic kinetic measurements for stereochemically nonrigid complexes of polyaromatic ligands with various transition metals and quantum chemical modeling of the behavior of such complexes seem to be topical to obtain an integral picture of dynamic processes in organoelement compounds.

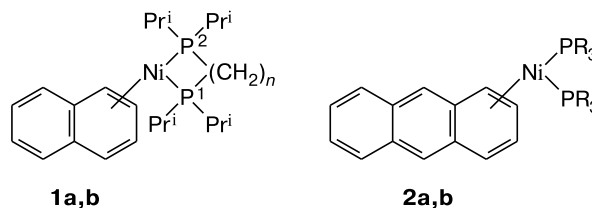
### Calculation Procedure

The molecular and transition-state geometries were optimized within the framework of DFT using the PBE functional<sup>33</sup> and the TZ2p full-electron, triple-zeta basis set of Gaussian functions.<sup>34,35</sup> The stationary points were identified by analyzing the Hessians. The energies (*E*) of the structures studied are reported with inclusion of zero-point vibrational energy corrections (ZPVE, *E*<sup>0</sup>). The Gibbs free energies *G* for *T* = 298.15 K were calculated using the statistical relations for a rigid rotator and harmonic oscillator. Correspondence between the transition states located and minima on the potential energy surfaces (PES) was established by constructing the intrinsic reaction coordinates (IRCs). All calculations were performed on an MVS-100k cluster at the Joint SuperComputer Center (JSCC) of the Russian Academy of Sciences (Moscow, Russia) using the PRIRODA-04 program.<sup>34</sup>

### Results and Discussion

**$\eta^2, \eta^2$ -Rearrangements of the (naphthalene and anthracene)nickel complexes.** We carried out DFT calculations of  $\eta^2, \eta^2$ -intra-ring HRs and  $\eta^2, \eta^2$ -inter-ring HRs in the 16e zero-valent ( $\eta^2$ -naphthalene and anthracene)nickel complexes. This type of fast reversible degenerate rearrangements proceeding consecutively as  $\eta^2, \eta^2$ -intra-ring HRs and  $\eta^2, \eta^2$ -inter-ring HRs was disclosed quite recently in studies of the (naphthalene<sup>20</sup> and anthracene<sup>36</sup>)nickel phosphine complexes. It was shown that the  $\eta^2$ -bound organometallic fragment migrates along the perimeter of the polyaromatic ligands.

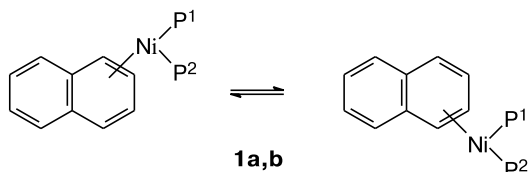
Reactions of metallacycles [(Pr<sup>i</sup>)<sub>2</sub>P(CH<sub>2</sub>)<sub>*n*</sub>P(Pr<sup>i</sup>)<sub>2</sub>]NiCl<sub>2</sub> (*n* = 2, 3) with naphthalene<sup>20</sup> or reactions of (R<sub>3</sub>P)<sub>2</sub>NiCl<sub>2</sub> (R = Et, Bu) with anthracene in the presence of magnesium in THF<sup>36</sup> result in the  $\eta^2$ -complexes **1a,b** and **2a,b** (determined from <sup>13</sup>C MAS NMR spectra). The <sup>13</sup>C NMR data were confirmed by the results of X-ray studies.<sup>37,38</sup>



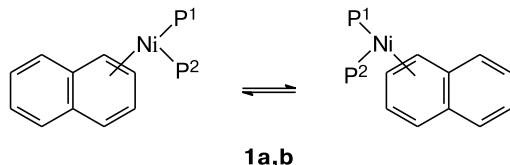
**1:** *n* = 2 (**a**), 3 (**b**)  
**2:** R = Et (**a**), Bu (**b**)

In complexes **1a,b**, the metallacycle  $P_2Ni$  quite rapidly migrates between the double bonds both within the same six-membered ring ( $\eta^2, \eta^2$ -intra-ring HR, Scheme 3) and between the rings ( $\eta^2, \eta^2$ -inter-ring HR, Scheme 4).

Scheme 3



Scheme 4



The activation barrier to the  $\eta^2, \eta^2$ -intra-ring HR (see Scheme 3) in complex **1a** in a solution in THF- $d_8$  is  $\Delta G^\ddagger = 5.4 \text{ kcal mol}^{-1}$ . This estimate is based on the line broadening in the  $^{13}C$  NMR spectrum. The activation energy of the process in the solid phase is much higher ( $\Delta G^\ddagger = 23 \text{ kcal mol}^{-1}$ ). This fact is illustrated by strong dependence of the thermodynamic parameters of haptotropic rearrangements on the aggregation state of the complexes.<sup>20</sup> The low  $\Delta G^\ddagger$  value for the solution agrees with the activation barriers to the  $\eta^2, \eta^2$ -intra-ring HRs in the cyclopolyolefin and arene complexes<sup>8–22</sup> mentioned above (see Scheme 1).

The  $\eta^2, \eta^2$ -inter-ring HR (see Scheme 4) in complex **1a** is observed only in solution and, according to 2D magnetization transfer  $^{13}C$  NMR spectra is characterized by a much higher activation energy  $\Delta G^\ddagger = 15 \text{ kcal mol}^{-1}$ ; this is also consistent with the general regularities of the inter-ring HRs compared to the intra-ring HRs (see Scheme 2).

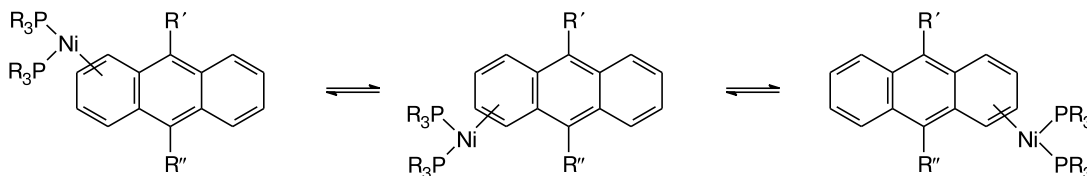
If the signals of phosphorus atoms in the  $^{31}P$  NMR spectrum of complex **1a** are averaged, the barrier to the

process is  $13 \text{ kcal mol}^{-1}$ , being somewhat lower than the barrier to the  $\eta^2, \eta^2$ -inter-ring HR. This is probably due to rotation of the nickel atom with its ligand environment about the axis perpendicular to the double bond, although other possible dynamic processes in the metallacycle (*e.g.*, ring inversion, a *flip-flop* reorientation, or the *windshield wiper* dynamics, *etc.*) cannot be ruled out.<sup>20</sup> In this case, the barrier to the process involving the averaging of the  $^{31}P$  NMR signals of two different phosphorus atoms approaches the barrier to rotation about the double bond in the  $L_2Ni$  fragment in the ethylene complex  $L_2Ni(C_2H_4)$ .<sup>39</sup> This provides additional arguments in favor that it is rotation of the Ni-phosphorus metallacycle about the axis perpendicular to the double bond that is responsible for the averaging of the signals of phosphorus atoms in complex **1a**.

Reactions of  $(R_3P)_2NiCl_2$  ( $R = Et, Bu$ ) in benzene with 9-alkyl- and 9,10-dialkylanthracenes ( $Alk = Me, Et$ ) (Scheme 5) resulted in the corresponding ( $\eta^2$ -anthracene) complexes,<sup>40</sup> which are structurally similar to complexes **2a,b**. Their structures were also determined by  $^{13}C$  MAS NMR experiments and confirmed by X-ray analysis.<sup>41</sup> As in complexes **2a,b**, the  $\eta^2, \eta^2$ -intra-ring HRs and  $\eta^2, \eta^2$ -inter-ring HRs were disclosed in all these anthracene complexes.

We studied the possibility for the  $\eta^2, \eta^2$ -intra-ring HR and  $\eta^2, \eta^2$ -inter-ring HR to occur in complex **2a** similarly to the case for complex **1a**. The  $^1H$  and  $^{13}C$  NMR spectra of complex **2a** in a solution of THF- $d_8$  suggested fast  $\eta^2, \eta^2$ -rearrangements involving migration of the organometallic group along the anthracene perimeter. The dynamic behavior of complex **2a** was studied by spin saturation transfer experiments and total lineshape analysis.  $^{13}C$  NMR experiments showed that, as in the naphthalene complexes, the organonickel group not only executes fast intra-ring migration ( $\Delta G^\ddagger \leq 4 \text{ kcal mol}^{-1}$ ), but also migrates from one terminal ring to the other by the intramolecular mechanism ( $\Delta H^\ddagger = 8 \text{ kcal mol}^{-1}$ ,  $\Delta S^\ddagger = -4.3$  entropy units,  $\Delta G^\ddagger \approx 15 \text{ kcal mol}^{-1}$ ). The intramolecular character of the process was proved by the absence of spin saturation transfer to free anthracene added to the reaction mixture. In some other organonickel derivatives of anthracene (see Scheme 5), the processes proceed by both the intramolecular and intermolecular mechanisms (experimental value is  $\Delta G^\ddagger = 15–17 \text{ kcal mol}^{-1}$ ).<sup>40</sup>

Scheme 5



$R = Et, Bu$ ;  $R' = H, Me, Et$ ;  $R'' = Me, Et$

To model the experimental results, we carried out a theoretical DFT study of the  $\eta^2, \eta^2$ -intra-ring HRs and  $\eta^2, \eta^2$ -inter-ring HRs in the nickel complexes of naphthalene **1a** and anthracene **2a**.

**Rearrangement in complex ( $\eta^2$ -C<sub>10</sub>H<sub>8</sub>)(dippe)Ni (**1a**).** Geometry optimization of the initial structure of the  $\eta^2$ -complex **1a** led to a global minimum on the PES, corresponding to the 16e zero-valent  $\eta^2$ -structure **1A** (Fig. 1) with the nickel atom coordinated to the carbon atoms of the C(1)—C(2) bond. Geometry optimization of another structure with the initial parameters taken from an X-ray study<sup>37</sup> of the crystals of complex **1a** led to structure **1B** whose energy and geometry are slightly different from those of **1A**.

In structure **1A**, the atoms C(1), C(2), Ni, P(1), and P(2) lie in the same plane; the distances are as follows: C(1)—Ni is 2.028 Å, C(2)—Ni is 2.017 Å, Ni—P(1) is 2.187 Å, and Ni—P(2) is 2.192 Å. The angle P(1)—Ni—P(2) is 92.3° and the angle C(1)—Ni—C(2) is 41.7°. The geometric parameters of structure **1B** almost coincide with those determined by X-ray analysis. Structurally, complexes **1A, B** are slightly different from complex **1a** (see Ref. 37) in mutual arrangement of isopropyl groups and in the metallacycle conformation.

Interconversion of structures **1A** and **1B** is possible by rotation of isopropyl groups accompanied by slight changes in the conformation of the metallacycle. Rotation can occur in two ways, as asynchronous process involving one isopropyl group or as concerted rotation of two isopropyl groups at phosphorus atoms. Both processes were theoretically modeled taking structure **1B** as an example. Calculations for rotation of isopropyl groups (one group for asynchronous process and two groups for concerted rotation) gave a number of rotamers with slightly different energies. The barriers to rotation are at most

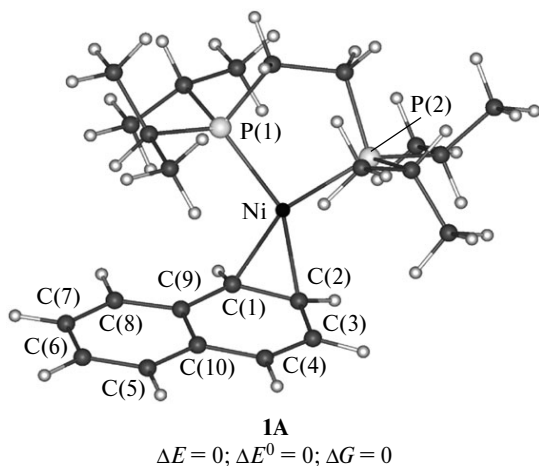
7 kcal mol<sup>−1</sup> in the former and about 10 kcal mol<sup>−1</sup> in the latter case.

Figure 2 presents the energies  $\Delta E^0$  of the rotamers **1B**, **1B-r1**, **1B-r2** and transition states **1B-rTS1**, **1B-rTS2**, **1B-rTS3** are plotted vs. angle  $\theta$  of asynchronous rotation of one isopropyl group. The structures of these rotamers and transition states are omitted because of low informativity. The Cartesian atomic coordinates and structures of all complexes, intermediates, and transition states studied in the present work within the framework of DFT are available on request.

One can construct the PES of concerted rotation of two, three, and four isopropyl groups in structures **1A** and **1B**. However, for the sake of simplicity we carried out calculations only for concerted rotation of two isopropyl groups in structure **1B** and obtained a higher barrier (see above) compared to the barrier to asynchronous rotation of one isopropyl group. This suggests that the latter mechanism is energetically more favorable for transitions of the system from one to another rotamer. In addition, this is accompanied by changes in the conformation of the metallacycle.

This low-barrier process seems to actually occur because no inequivalence of carbon atoms of isopropyl groups in the <sup>13</sup>C solid-state NMR spectra and signal broadening in the high-resolution NMR spectra were observed even at very low temperatures.<sup>20</sup> However, the contribution of concerted rotation of several isopropyl groups to the overall dynamic behavior of complex cannot be completely excluded because the barrier to this process is only 3 kcal mol<sup>−1</sup> higher than the barrier to asynchronous rotation.

According to calculations, the  $\eta^2, \eta^2$ -intra-ring HR in isomer **1A** proceeds with a low barrier  $\Delta G^\ddagger = 4.2$  kcal mol<sup>−1</sup> via a nonplanar 18e  $\eta^4$ -*cis*-butadiene transition state **1A-TS1** (distances from the nickel atom to the C(1), C(2), C(3), and C(4) atoms are 2.267, 2.023, 2.123, and 2.493 Å, respectively, and the corresponding bond orders are 0.35, 0.46, 0.34, and 0.31). The dihedral angle between the almost planar butadiene moiety (the C(1)—C(4) axis deviates from the plane by 2–3°) and the rest part of the ligand



**Fig. 1.** Optimized structure **1A** of the complex ( $\eta^2$ -C<sub>10</sub>H<sub>8</sub>)-(dippe)Ni (**1a**). Here and in Figs 2–7 the parameters  $\Delta E$ ,  $\Delta E^0$ , and  $\Delta G$  are given in kcal mol<sup>−1</sup>.

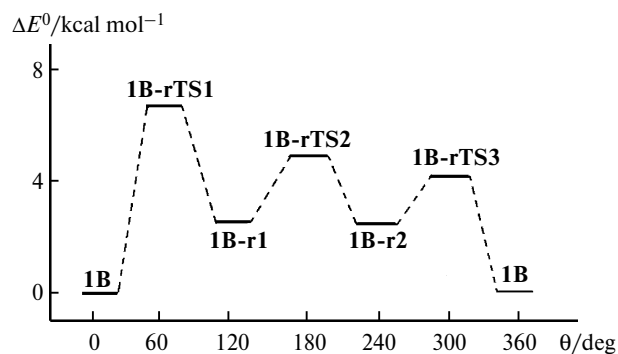


**Fig. 2.** Total energy plotted vs. angle of rotation ( $\theta$ ) of one isopropyl group in structure **1B** of the complex **1a**.

is 20.3°, being close to 26.2° for the 18e ( $\eta^4$ -anthracene) complex of zero-valent nickel.<sup>42</sup> These results suggest that the transition state **1A-TS1** has a  $\eta^4$ -structure (Fig. 3) and that the rearrangement is described by the scheme **1A**  $\rightarrow$  **1A-TS1**  $\rightarrow$  **1C**. Complexes **1C** and **1A** are structurally similar and have close energies. The  $\eta^2, \eta^2$ -intra-ring HR in structure **1B** proceeds *via* a similar  $\eta^4$ -*cis*-butadiene transition state **1B-TS1** ( $\Delta G^\ddagger = 4.7$  kcal mol<sup>-1</sup>,  $\Delta G^\ddagger_{\text{exp}} = 5.4$  kcal mol<sup>-1</sup> (see Ref. 20)) as follows: **1B**  $\rightarrow$  **1B-TS1**  $\rightarrow$  **1D**.

Earlier,<sup>43</sup> the results of EHT calculations suggested that the  $\eta^2, \eta^2$ -intra-ring HR in the complex [Ni( $\eta^2$ -C<sub>6</sub>(CF<sub>3</sub>)<sub>6</sub>)(CO)<sub>2</sub>] proceeds *via* a  $\eta^3$ -transition state. However, in more recent studies the structure of the transition states of the  $\eta^2, \eta^2$ -intra-ring HRs in zero-valent nickel complexes with arenes (see Scheme 1) were revised and the transition states were ascribed a  $\eta^4$ -hapticity<sup>44</sup> as for the transition state of the  $\eta^2, \eta^2$ -intra-ring HRs in the structurally similar  $\eta^2$ -complexes of COT.<sup>14</sup>

According to our DFT calculations, the  $\eta^2, \eta^2$ -intra-ring HRs in structures **1A** and **1B** result in the complexes **1C** and **1D**, respectively, which are slightly different in energy from each other and from the initial complexes **1A** and **1B** owing to different mutual arrangement of bulky isopropyl groups and different conformations of the metallacycle.

Structures **1C** and **1D** can be obtained from the initial structures **1A** and **1B** by rotating isopropyl groups and changing the metallacycle conformation. However, calculations of these processes would significantly complicate the pattern of activation of the rearrangements in question without changing it fundamentally. Therefore, no special DFT calculations of the energy changes due to conformational mobility of the metallacycle were performed. Since no broadening of the signals of the corresponding ring protons in the low-temperature NMR spectra of complex **1a** were observed,<sup>20</sup> it follows that such

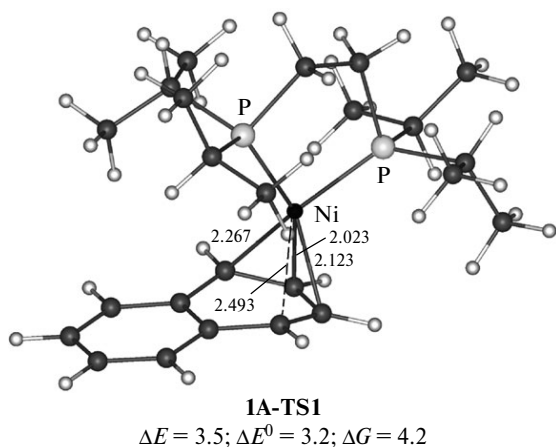


**Fig. 3.** Transition state **1A-TS1** of the  $\eta^2, \eta^2$ -intra-ring HR **1A**  $\rightarrow$  **1A-TS1**  $\rightarrow$  **1C**. Here and in Figs 5 and 7 the distances are given in Å.

changes should be at most a few kcal mol<sup>-1</sup>, as for rotation of isopropyl groups. In addition, structures **1C**, **1D** and **1A**, **1B**, respectively, are almost mirror symmetric relative to the mid-points of the C(2)–C(3), C(9)–C(10), and C(6)–C(7) bonds (atomic numbering scheme for the naphthalene ligand is shown in Fig. 1).

The  $\eta^2, \eta^2$ -inter-ring HRs were studied for structures **1A** and **1B**. In structure **1A**, the process proceeds along the periphery of the aromatic ligand *via* a  $\eta^3$ -allylic transition state **1A-TS2** (Fig. 4), as unambiguously indicated by the distances from the Ni atom to the atoms C(8), C(9), C(1), and C(10) equal to 2.246, 2.044, 2.237, and 2.978 Å, respectively. The inter-ring HR **1A**  $\rightarrow$  **1A-TS2**  $\rightarrow$  **1E** with the activation barrier  $\Delta G^\ddagger = 12.2$  kcal mol<sup>-1</sup> results in complex **1E**. The experimental activation barrier obtained from spin saturation transfer 2D <sup>13</sup>C NMR experiments is  $\Delta G^\ddagger_{\text{exp}} = 15$  kcal mol<sup>-1</sup>, being somewhat higher than the theoretical one.<sup>20</sup>

The activation pattern of the  $\eta^2, \eta^2$ -inter-ring HR significantly complicates for the complex **1B** (**1B**  $\rightarrow$  **1B-TS2**  $\rightarrow$  **1B-IM**  $\rightarrow$  **1B-TS3**  $\rightarrow$  **1F**) (complexes **1F** and **1B**, as well as complexes **1A** and **1E**, have different energies; the reasons were discussed above for the structures **1A–1D**). In addition to the high-lying  $\eta^3$ -transition state **1B-TS2** ( $\Delta G = 12.4$  kcal mol<sup>-1</sup>), which is almost identical to the transition state **1A-TS2**, a structurally similar  $\eta^2$ -intermediate **1B-IM** ( $\Delta G = 9.7$  kcal mol<sup>-1</sup>) and a  $\eta^2$ -transition state **1B-TS3** ( $\Delta G = 11.0$  kcal mol<sup>-1</sup>) lying lower in energy than structure **1B-TS2** were located.

The overall activation barrier to the  $\eta^2, \eta^2$ -inter-ring HR in structure **1B** is determined by the transition state

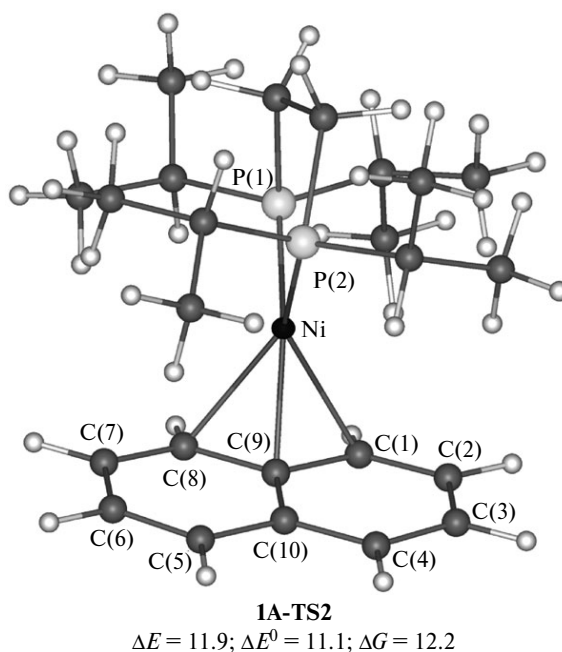


**Fig. 4.** Transition state **1A-TS2** of the  $\eta^2, \eta^2$ -inter-ring HR **1A**  $\rightarrow$  **1A-TS2**  $\rightarrow$  **1E**.

**1B-TS2** characterized by the maximum energy  $\Delta G = 12.4 \text{ kcal mol}^{-1}$ . Despite a qualitative difference and complexity of the process, the activation pattern of the  $\eta^2, \eta^2$ -inter-ring HR in structure **1B** quantitatively remains almost the same as that of the  $\eta^2, \eta^2$ -inter-ring HR in structure **1A** and reasonably describes the experimental results.

The calculated activation barriers to the  $\eta^2, \eta^2$ -inter-ring HRs in structures **1A** and **1B** are close, although about  $3 \text{ kcal mol}^{-1}$  lower than the value determined by NMR spectroscopy. It should be noted that experiments were carried out in solution, whereas calculations were performed for the gas phase.

Neither  $\eta^2, \eta^2$ -intra-ring nor  $\eta^2, \eta^2$ -inter-ring HRs in structures **1A** and **1B** cause exchange of phosphorus atoms, which, according to  $^{31}\text{P}$  NMR experimental data, corresponds to a barrier of  $13 \text{ kcal mol}^{-1}$ . We calculated the PES for rotation of the Ni(dippe) (dippe is 1,2-bis(diisopropylphosphino)ethane) fragment about the axis passing through the mid-point of the C(1)—C(2) bond of the naphthalene ligand in structure **1B**. An analysis shows that this process leads to exchange of phosphorus atoms in structure **1B**, i.e., signal averaging in the  $^{31}\text{P}$  NMR spectrum should be observed. Rotation of the metallacycle about the double bond in complex **1B**, which causes the averaging of phosphorus atoms, proceeds *via* the transition state **1B-TS4** with the activation barrier  $\Delta G^\ddagger = 12.3 \text{ kcal mol}^{-1}$  and results in the  $\eta^2$ -complex **1G** (**1B**  $\rightarrow$  **1B-TS4**  $\rightarrow$  **1G**).

The activation barrier is close to the experimentally determined one ( $\Delta G^\ddagger = 13 \text{ kcal mol}^{-1}$ ). It is characteristic of rotation of the organometallic fragment in nickel  $\eta^2$ -complexes with olefins.<sup>39</sup> Complexes **1B** and **1G** have different energies. As for the complexes **1A**—**1F** (see above), equalization of the energies of the initial and final complexes requires further rotation of isopropyl groups and minor changes in the metallacycle conformation.

**Haptotropic rearrangements in (anthracene)nickel complex 2a. Intra-ring haptotropic rearrangement ( $\eta^2, \eta^2$ -intra-ring HR).** DFT calculations of complex **2a** with ethyl substituents at the phosphorus atoms were carried out using the  $\eta^2$ -structure **2A** (Fig. 5,a) as the initial approximation. In this structure, the Ni atom is coordinated to the C(1) and C(2) atoms (the distances C(1)—Ni and C(2)—Ni are 2.068 and 2.004 Å, respectively) The predicted structure agrees with the X-ray data.<sup>41</sup> This complex undergoes a rearrangement ( $\eta^2, \eta^2$ -intra-ring HR) to a structurally similar  $\eta^2$ -complex **2B** with the metal atom coordinated to the C(3) and C(4) atoms and a close energy. The rearrangement **2A**  $\rightarrow$  **2-TS1**  $\rightarrow$  **2B** proceeds *via* the  $\eta^4$ -*cis*-butadiene transition state **2-TS1** (Fig. 5,b) with  $\eta^4$ -coordination to the C(1), C(2), C(3), and C(4) atoms, which is similar to the transition states of the naphthalene complex **1A-TS1** and **1B-TS1**. The six-membered ring is folded along the C(1)—C(4) line. The dihedral angle is  $18.4^\circ$ . The calculated activation energy of this process

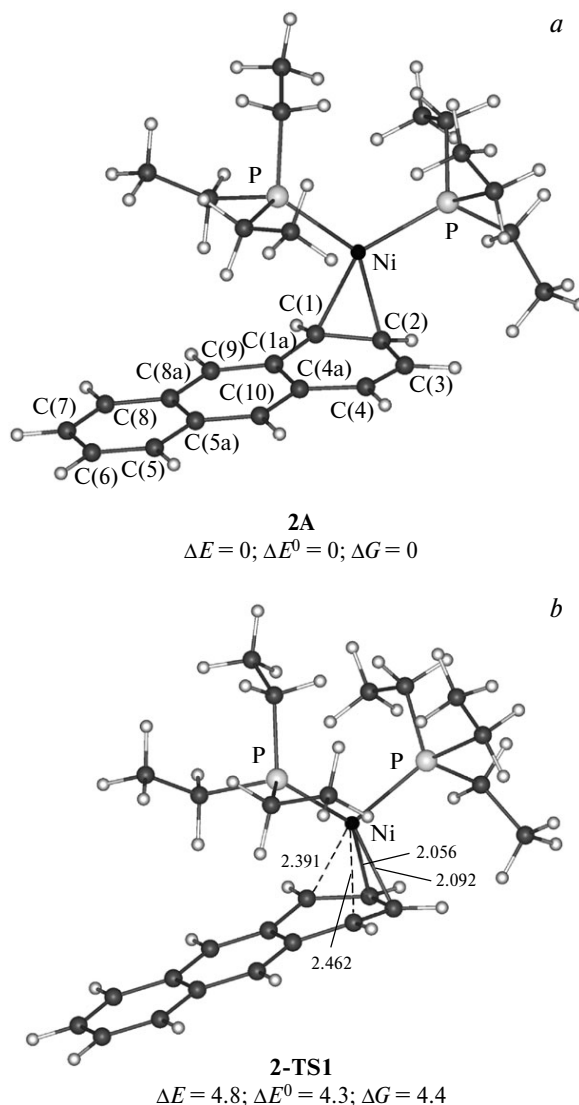
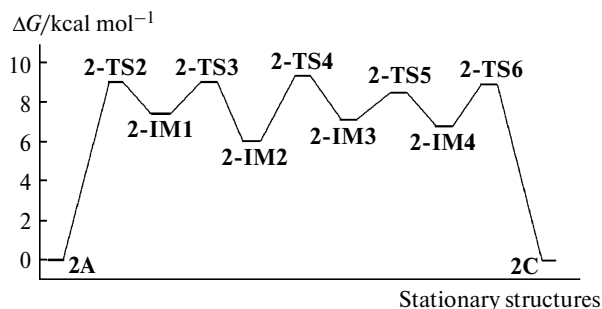


Fig. 5. Structures and energies of the stationary states corresponding to the stationary points on the PES of the  $\eta^2, \eta^2$ -intra-ring HR **2A**  $\rightarrow$  **2-TS1**  $\rightarrow$  **2B**.

( $4.4 \text{ kcal mol}^{-1}$ ) agrees with the experimentally determined value ( $\Delta G^\ddagger \leq 4 \text{ kcal mol}^{-1}$ ).

**Inter-ring haptotropic rearrangement ( $\eta^2, \eta^2$ -inter-ring HR).** According to calculations, the intramolecular  $\eta^2, \eta^2$ -inter-ring HR in complex **2a** proceeds in a more complicated way than in complex **1a**, but the organometallic fragment also migrates along the periphery of the polycyclic ligand in the course of the rearrangement. Five transition states and four intermediates were located on the PES, namely, **2A**  $\rightarrow$  **2-TS2**  $\rightarrow$  **2-IM1**  $\rightarrow$  **2-TS3**  $\rightarrow$  **2-IM2**  $\rightarrow$  **2-TS4**  $\rightarrow$  **2-IM3**  $\rightarrow$  **2-TS5**  $\rightarrow$  **2-IM4**  $\rightarrow$  **2-TS6**  $\rightarrow$  **2C** (Fig. 6).

As in the case of the naphthalene complexes, the energy characteristics of the  $\eta^2$ -anthracene complexes **2C** and **2A** are slightly different. To perform no additional calcu-



**Fig. 6.** Energy diagram of the  $\eta^2, \eta^2$ -inter-ring HR  $2A \rightarrow 2-TS2 \rightarrow 2-IM1 \rightarrow 2-TS3 \rightarrow 2-IM2 \rightarrow 2-TS4 \rightarrow 2-IM3 \rightarrow 2-TS5 \rightarrow 2-IM4 \rightarrow 2-TS6 \rightarrow 2C$ .

lations that do not change the overall activation pattern, no geometry optimization of the  $\eta^2$ -rotamer by rotating ethyl groups was carried out. It should also be taken into account that the  $\eta^2, \eta^2$ -inter-ring HR is fully reversible; in this connection, the distinctions between complexes **2A** and **2C** seem to be insignificant.

The highest theoretically predicted activation energy of the overall process is  $9.3 \text{ kcal mol}^{-1}$  (**2-TS4**, Fig. 7), being lower than the experimental value  $\Delta G^\ddagger_{\text{exp}} \approx 15 \text{ kcal mol}^{-1}$  ( $\Delta H^\ddagger = 13.6 \text{ kcal mol}^{-1}$ ,  $\Delta S^\ddagger = -4.3$  entropy units), as determined from the total lineshape analysis of the dynamic NMR spectra.<sup>38</sup> Intra- and intermolecular  $\eta^2, \eta^2$ -inter-ring HR in related (9,10-dimethyl- and 9,10-diethylanthracene)nickel complexes (see Scheme 5) have similar experimental activation energies  $\Delta G^\ddagger \approx 15 \text{ kcal mol}^{-1}$ .<sup>40</sup>

The rearrangements were conducted in THF- $d_8$ , a polar solvent appropriate for solvation of organometallic fragments.<sup>20,38,40</sup> This was probably the reason why the  $\eta^2, \eta^2$ -

inter-ring HRs in some complexes could proceed by the intermolecular dissociative mechanism involving abstraction of the organonickel group from the aromatic ligand. This is indicated by rather high negative values of the entropy of activation.

It cannot be ruled out that an increase in the experimental activation barrier in the case of complexes **1a** and **2a** is due to partial cleavage or weakening of  $\pi$ -bonds upon coordination of additional THF molecules in the course of the rearrangement (solvation mechanism), which requires additional energy expenditure. However, this mechanism seems to be improbable. In the case of the anthracene complexes (see Scheme 5), steric hindrance produced by the alkyl substituents in positions C(9) and C(10) of anthracene when the organometallic fragment migrates along the periphery of the aromatic ligand can also lead to an increase in the activation barrier. There reasons, although less probable, as well as the dissociative mechanism itself, can lead to an increase in the barrier to the  $\eta^2, \eta^2$ -inter-ring HR.

When needed, the intramolecular character of the process was additionally proved by the absence of spin saturation transfer to the free aromatic ligand or organonickel group.<sup>20,38,40</sup> In such cases, even minor contributions from the intermolecular dissociative mechanism (as the main additional mechanism) to the intramolecular  $\eta^2, \eta^2$ -inter-ring HR can, in principle, lead to an increase in the activation barrier  $\Delta G^\ddagger$  for both the naphthalene and anthracene complexes.

The hapticity of stationary states corresponding to stationary points on the PES, *i.e.*, the number of carbon atoms of the polyaromatic ligand bound to the metal atom (M) may be of special interest. When considering stable complexes, the presence of M—C bonds is usually indicated by the corresponding distances (X-ray data).<sup>37,41</sup> Other M—C bond criteria can serve the  $^1\text{H}$  and  $^{13}\text{C}$  NMR spectral parameters, the chemical shift being the main one. For instance, in the  $^{13}\text{C}$  NMR spectra, the chemical shifts of the carbon atoms bound to the metal atom M are usually smaller and in the high-field region, whereas in the  $^1\text{H}$  NMR spectra,<sup>45</sup> signals of the protons bound to these carbon atoms are shifted downfield.

NMR spectroscopy and X-ray analysis are inapplicable to intermediates and transition states. It was proposed<sup>24</sup> to determine the hapticity using the bond order as a criterion (usually, the bond order correlates with the bond length). The data of Table 1 show that the M—C bond order does not always correlate with the distance  $d(\text{M—C})$ . Such cases deserve particular consideration.

The hapticity values of the stationary states of the  $\eta^2, \eta^2$ -intra-ring HR were determined unambiguously, *viz.*,  $\eta^2$  for structures **2A** and **2B** and  $\eta^4$  for the transition state **2-TS1**, because the bond orders correlate with the distances  $d(\text{M—C})$ . In the case of the  $\eta^2, \eta^2$ -inter-ring HR, the situation is complicated by the fact that the rearrange-

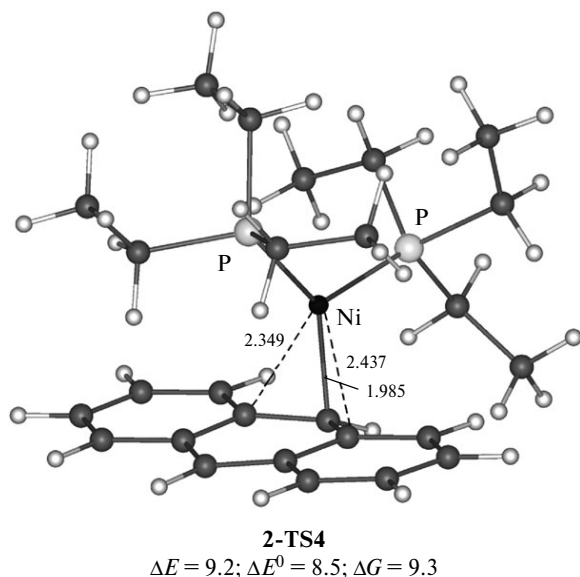


**Fig. 7.** Structure of the highest-lying  $\eta^3$ -transition state **2-TS4** of the  $\eta^2, \eta^2$ -inter-ring HR in structure **2A**.

**Table 1.** C—Ni bond orders (according to Mulliken), C—Ni bond lengths, the chemical shifts (CS) of C atoms in theoretical  $^{13}\text{C}$  NMR spectra, and the hapticities of the structures of haptotropic rearrangements in complex **2A**

Structure	Hapticity	Atom C	Bond order C—Ni	Bond length C—Ni, d/Å	CS, $\delta$ , ppm	Structure	Hapticity	Atom C	Bond order C—Ni	Bond length C—Ni, d/Å	CS, $\delta$ , ppm
<b>2A</b>	$(\eta^2)$	C(1)	0.48	2.068	69.8	<b>2-TS4</b>	$(\eta^3)$	C(1a)	0.14	2.437	110.1
		C(2)	0.48	2.004	68.7			C(9)	0.57	1.985	69.4
		C(3)	0.10	2.753	129.9*			C(8a)	0.18	2.349	102.9
		C(4)	0.11	3.406	127.4*			C(8)	0.15	3.053	133.4*
<b>2-TS1</b>	$(\eta^4)$ <i>cis</i> -butadiene	C(1)	0.34	2.391	91.2	<b>2-IM3</b>	$(\eta^3)$	C(1a)	0.11	2.881	130.9*
		C(2)	0.37	2.056	86.4			C(9)	0.55	2.046	64.9
		C(3)	0.35	2.092	87.9			C(8a)	0.25	2.110	91.0
		C(4)	0.29	2.462	98.7			C(8)	0.19	2.576	116.1
<b>2B</b>	$(\eta^2)$	C(1)	0.12	3.404	128.0*	<b>2-TS5</b>	$(\eta^3)$	C(9)	0.46	2.228	71.7
		C(2)	0.09	2.765	129.7*			C(8a)	0.15	2.077	93.3
		C(3)	0.51	2.008	66.3			C(8)	0.40	2.257	85.3
		C(4)	0.47	2.068	67.7			C(5a)	0.15	3.050	140.3*
<b>2-TS2</b>	$(\eta^4)$ <i>trans</i> -butadiene	C(1)	0.51	2.023	75.6	<b>2-IM4</b>	$(\eta^4)$ <i>trans</i> -butadiene	C(9)	0.34	2.372	86.2
		C(2)	0.24	2.648	102.1			C(8a)	0.19	2.084	94.3
		C(1a)	0.19	2.158	96.6			C(8)	0.46	2.124	76.7
		C(9)	0.24	2.632	107.0			C(7)	0.20	2.933	114.1
<b>2-IM1</b>	$(\eta^4)$ <i>trans</i> -butadiene	C(1)	0.47	2.086	76.0	<b>2-TS6</b>	$(\eta^4)$ <i>trans</i> -butadiene	C(9)	0.18	2.746	112.5
		C(2)	0.20	2.849	111.1			C(8a)	0.19	2.196	100.1
		C(1a)	0.18	2.102	94.1			C(8)	0.55	1.998	74.8
		C(9)	0.34	2.446	94.1			C(7)	0.31	2.517	95.1
<b>2-TS3</b>	$(\eta^4)$	C(1)	0.42	2.181	79.1	<b>2C</b>	$(\eta^2)$	C(8a)	0.09	3.056	145.3*
		C(2)	0.16	3.037	117.2			C(8)	0.47	2.070	69.1
		C(1a)	0.15	2.081	93.2			C(7)	0.48	2.006	68.4
		C(9)	0.46	2.302	82.0			C(6)	0.07	2.813	131.0*
<b>2-IM2</b>	$(\eta^3)$	C(1)	0.19	2.547	112.6						
		C(1a)	0.23	2.102	93.0						
		C(9)	0.49	2.065	67.2						
		C(8a)	0.15	2.919	131.1*						

\* The final hapticity was ascribed to a structure taking into account the CS indicating the lack of the bond between the metal atom and the given carbon atom.

ment proceeds at the periphery of the anthracene ring near the carbon atoms that form two inner C—C bonds, C(1a)—C(4a) and C(8a)—C(5a), whose  $\pi$ -electrons are much less involved in the coordination bonding with the metal atom. For instance, in structure **2-TS2**, despite the short distance Ni—C(1a) (2.158 Å), the order of this bond is 0.19 (see Table 1), being 0.05 smaller than for the atoms C(2) and C(9) for which the corresponding distances are about 0.5 Å longer.

Therefore, the  $\eta^4$  can be ascribed to the transition state **2-TS2** only with some restrictions. The hapticities of the structures **2-IM1**, **2-TS3**, **2-IM2**, **2-TS4**, **2-TS5**, **2-IM4**, and **2-TS6** are also determined ambiguously. It should be noted that exact determination of the hapticity of transition states and intermediates is not necessary and is needed only for clarity in the description of the reaction mechanism.

Interestingly, the calculated chemical shifts in the  $^{13}\text{C}$  NMR spectra can also be useful for hapticity estimation

and making final decisions in doubtful cases. An upfield shift from the value  $\delta$  128 corresponding to the signal of benzene carbon atoms in the  $^{13}\text{C}$  NMR spectrum may be an indication of a carbon—metal bond and suggests a quite reliable determination of the hapticity of the corresponding structure.

Summing up, the  $\eta^2, \eta^2$ -intra-ring and  $\eta^2, \eta^2$ -inter-ring HRs in the (naphthalene and anthracene)nickel complexes were studied within the framework of the DFT approach. The  $\eta^2, \eta^2$ -intra-ring HRs proceed *via* the  $\eta^4$ -*cis*-butadiene transition states, whereas the  $\eta^2, \eta^2$ -inter-ring HRs proceed *via* high-lying  $\eta^3$ -allylic transition states. The hapticities of the intermediates and transition states are higher than those of the corresponding neutral zero-valent 16e  $\eta^2$ -complexes. The calculated activation barriers to the  $\eta^2, \eta^2$ -intra-ring HRs in the nickel complexes of naphthalene and anthracene and the barrier to rotation of the organonickel group about the double bond in the

former complex approach the corresponding experimental values. The predicted barriers to the  $\eta^2, \eta^2$ -inter-ring HRs are somewhat lower than the experimental values. A possible explanation is that the experimental values were determined for complexes in the polar solvent in which the process may also proceed by the intermolecular dissociative mechanism, whereas the theoretical values were obtained for the  $\eta^2, \eta^2$ -inter-ring HRs proceeding by the intramolecular mechanism in the gas phase.

The authors express their gratitude to the Alexander von Humboldt Foundation (Bonn, Germany) for providing a workstation and auxiliary hardware for DFT calculations.

### References

1. I. D. Gridnev, O. L. Tok, in *Fluxional Organometallic and Coordination Compound*, Eds M. Gielen, R. Willem, B. Wrackmeyer, John Wiley and Sons, Chichester, 2004, vol. 4, p. 41.
2. C. H. Bartholomew, R. J. Farrauto, *Fundamentals of Industrial Catalytic Processes*, Wiley-Interscience, Hoboken, 2006, 966 pp.
3. K. Weissmehl, H.-J. Arpe, *Industrial Organic Chemistry*, Wiley-VCH, Weinheim, 2003, 511 pp.
4. I. Bach, K.-R. Pörschke, R. Goddard, C. Kopiske, C. Krüger, A. Ruffińska, K. Seevogel, *Organometallics*, 1996, **15**, 4959.
5. Yu. F. Oprunenko, *Usp. Khim.*, 2000, **69**, 744 [*Russ. Chem. Rev. (Engl. Transl.)*, 2000, **69**, 683].
6. Yu. Oprunenko, I. Gloriovzov, K. Lyssenko, S. Malyugina, D. Mityuk, V. Mstislavsky, H. Günther, G. von Firks, M. Ebener, *J. Organomet. Chem.*, 2002, **656**, 27.
7. M. V. Zabalov, I. P. Gloriovzov, Yu. F. Oprunenko, D. A. Lemenovskii, *Izv. Akad. Nauk, Ser. Khim.*, 2003, 1484 [*Russ. Chem. Bull., Int. Ed.*, 2003, **52**, 1567].
8. I. Gridnev, *Coord. Chem. Rev.*, 2008, **252**, 1798.
9. F. A. Cotton, *Acc. Chem. Res.*, 1968, **1**, 257.
10. I. D. Gridnev, N. U. Zhanpeisov, M. K. C. del Rosario, *J. Phys. Chem. B*, 2005, **109**, 12498.
11. I. B. Benson, S. A. R. Knox, R. F. D. Stansfield, P. Woodward, *J. Chem. Soc., Dalton Trans.*, 1981, 51.
12. A. Cutler, D. Ehntholt, W. P. Giering, P. Lennon, S. Raghu, A. Rosan, M. Rosenblum, J. Tancrede, D. Wells, *J. Am. Chem. Soc.*, 1976, **98**, 3495.
13. M. S. Lawless, D. S. Marynick, *J. Am. Chem. Soc.*, 1991, **113**, 7513.
14. I. Bach, K.-R. Pörschke, B. Proft, R. Goddard, C. Kopiske, C. Krüger, A. Ruffińska, K. Seevogel, *J. Am. Chem. Soc.*, 1997, **119**, 3373.
15. K. J. Karel, T. A. Albright, M. Brookhart, *Organometallics*, 1982, **1**, 419.
16. D. R. Muhandiram, G. Y. Kiel, G. H. M. Aarts, I. M. Saez, J. G. A. Reuvers, D. M. Heinekey, W. A. G. Graham, J. Takats, R. E. D. McClung, *Organometallics*, 2002, **21**, 2687.
17. W. D. Harman, H. Taube, *J. Am. Chem. Soc.*, 1987, **109**, 1883.
18. L. Cronin, C. L. Higgitt, R. N. Perutz, *Organometallics*, 2000, **19**, 672.
19. H. van der Heijden, A. G. Orpen, P. Pasman, *J. Chem. Soc., Chem. Commun.*, 1985, 1576.
20. R. Benn, R. Mynott, I. Topalović, F. Scott, *Organometallics*, 1989, **8**, 2299.
21. W. D. Jones, M. G. Partridge, R. N. Perutz, *J. Chem. Soc., Chem. Commun.*, 1991, 264.
22. T. W. Bell, M. Helliwell, W. D. Jones, M. G. Partridge, R. N. Perutz, *Organometallics*, 1992, **11**, 1911.
23. Yu. F. Oprunenko, DSc Thesis (Chem.), M. V. Lomonosov Moscow State Univ., Moscow, 1999 (in Russian).
24. Y. F. Oprunenko, I. P. Gloriovzov, *J. Organomet. Chem.*, 2009, **694**, 1195.
25. O. Joistgen, A. Pfletschinger, J. Ciupka, M. Dolg, M. Niegler, G. Schnakenburg, R. Fröhlich, O. Kataeva, K.-H. Dötz, *Organometallics*, 2009, **28**, 3473.
26. L. Turker, S. Gumus, *Acta Chim. Slov.*, 2009, **56**, 246.
27. J. Li, H. Li, X. Liang, S. Zhang, T. Zhao, D. Xia, Z. Wu, *J. Phys. Chem. A*, 2009, **113**, 791.
28. M. L. H. Green, A. H. H. Stephens, *Chem. Commun.*, 1997, 793.
29. L. N. Novikova, B. A. Mazurchik, Yu. F. Oprunenko, N. A. Ustynyuk, *Izv. Akad. Nauk, Ser. Khim.*, 2001, 151 [*Russ. Chem. Bull., Int. Ed.*, 2001, **50**, 157].
30. E. Kirillov, S. Kahlal, T. Roisnel, T. Georgelin, J.-Y. Sallard, J.-F. Carpentier, *Organometallics*, 2008, **27**, 387.
31. R. H. Crabtree, C. P. Parnell, *Organometallics*, 1984, **3**, 1727.
32. Yu. F. Oprunenko, I. P. Gloriovzov, *Izv. Akad. Nauk, Ser. Khim.*, 2010, 2008 [*Russ. Chem. Bull., Int. Ed.*, 2010, **59**, No. 11].
33. J. P. Perdew, K. Burke, M. Ernzerhof, *Phys. Rev. Lett.*, 1996, **77**, 3865.
34. D. N. Laikov, *Chem. Phys. Lett.*, 1997, **281**, 151.
35. D. N. Laikov, Yu. A. Ustynyuk, *Izv. Akad. Nauk, Ser. Khim.*, 2005, 805 [*Russ. Chem. Bull., Int. Ed.*, 2005, **54**, 820].
36. A. Stanger, *Organometallics*, 1991, **10**, 2979.
37. F. Scott, C. Krüger, P. Betz, *J. Organomet. Chem.*, 1990, **387**, 113.
38. A. Stanger, K. P. C. Vollhardt, *Organometallics*, 1992, **11**, 317.
39. (a) C. Krüger, Y. H. Tsay, *J. Organomet. Chem.*, 1972, **34**, 387; (b) R. Benn, *Org. Magn. Reson.*, 1983, **21**, 723.
40. A. Stanger, H. Weismann, *J. Organomet. Chem.*, 1996, **515**, 183.
41. A. Stanger, R. Boese, *J. Organomet. Chem.*, 1992, **430**, 235.
42. R. Boese, A. Stanger, P. Stellberg, A. Shazar, *Angew. Chem., Int. Ed.*, 1993, **32**, 1475.
43. J. Silvestre, T. A. Albright, *J. Am. Chem. Soc.*, 1985, **107**, 6829.
44. T. Braun, L. Cronin, C. L. Higgitt, J. E. McGrady, R. N. Perutz, M. Reinhold, *New J. Chem.*, 2001, **25**, 19.
45. Ch. Elschenbroich, *Organometallics*, 3rd ed., Wiley-VCH, Weinheim, 2006, 804 pp.

Received June 3, 2010;  
in revised form December 29, 2010